Electronic Supplementary Material (ESI) for Journal of Materials Chemistry B.

Supplementary information

CT/NIRF dual-modal imaging tracking and therapeutic efficacy of transplanted mesenchymal stem cells labeled with Au nanoparticles in silica-induced pulmonary fibrosis

Authors: Huang, Huang, Ning, Luo, Chen, Wang, Zhang, Zhang, Chao

Table of contents

Supplementary Table S1

qRT-PCR primers		
Gene	**Forward (5′-3′)**	**Reverse (5′-3′)**
GAPDH (mouse)	**TGTGTCCGTCGTGGATCTGA**	**CCTGCTTCACCACCTTCTTGA**
TNF-α (mouse)	**CAGGCGGTGCCTATGTCTC**	**CGATCACCCCGAAGTTCAGTAG**
IL-6 (mouse)	**CTGCAAGAGACTTCCATCCAG**	**AGTGGTATAGACAGGTCTGTTGG**
CXCL2 (mouse)	**GCGCCCAGACAGAAGTCATAG**	**GGCAAACTTTTTGACCGCC**

Supplementary Figure S1

A.

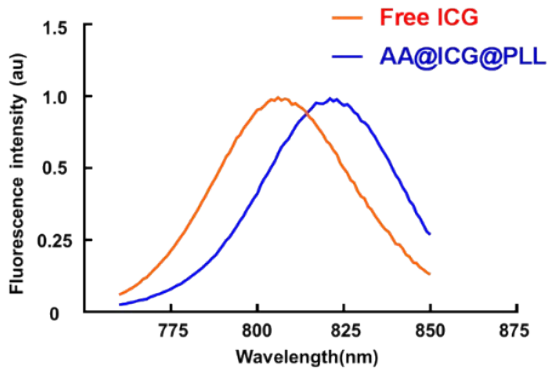

B.

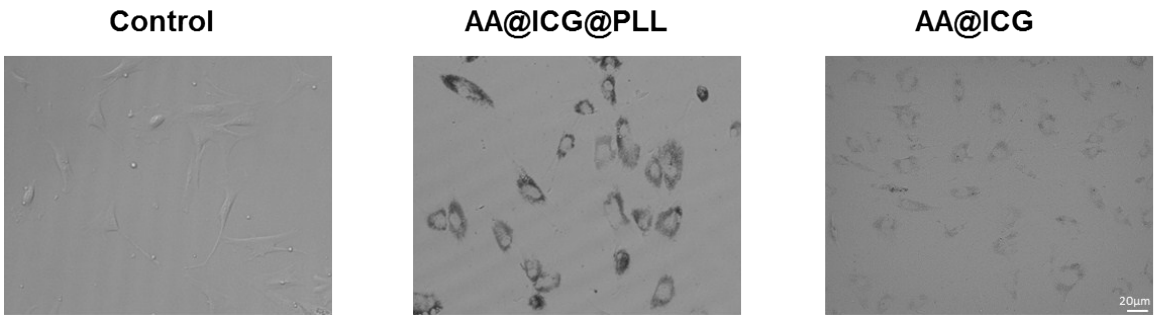

C.

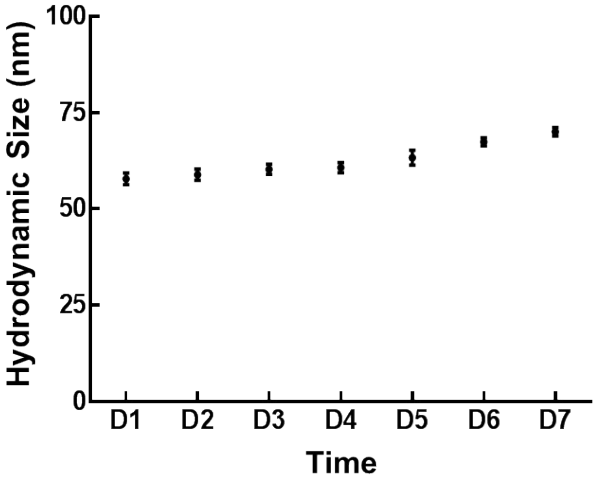

D.

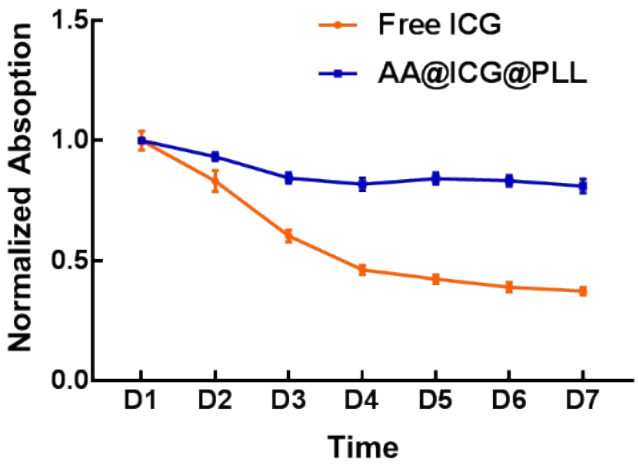

Figure S1. Characterization of AA@ICG@PLL NPs

A. Fluorescence spectra of free ICG and AA@ICG@PLL. **B.** Bright-field images of blank MSCs and MSCs incubated with AA@ICG or AA@ICG@PLL. Scale bar=20 μm. **C.** Hydrodynamic size change of AA@ICG@PLL in one week. **D.** Measurement of the absorption spectra of free ICG and AA@ICG@PLL in one week.

Supplementary Figure S2

A.

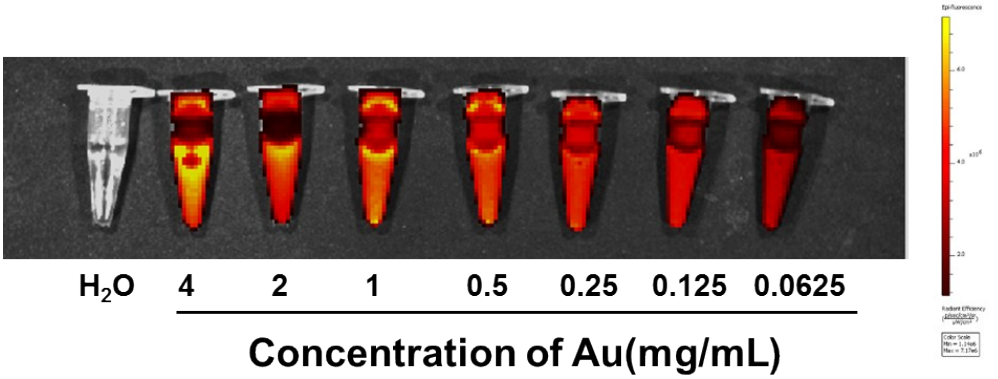

B.

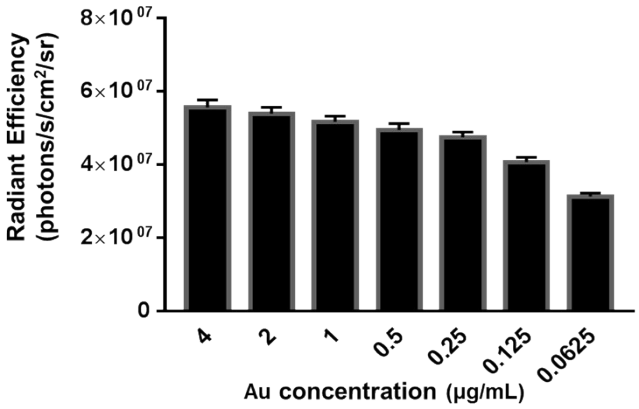

Figure S2. *In vitro* NIR fluorescence images of AA@ICG@PLL NPs with different Au concentrations.

A. *In vitro* fluorescence images of AA@ICG@PLL NPs with different Au concentrations. **B.** The total radiant efficiency of AA@ICG@PLL NPs with different Au concentrations is shown in the bar chart.

Supplementary Figure S3

A.

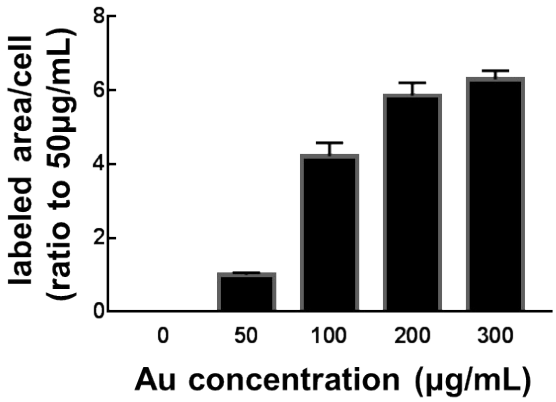

B.

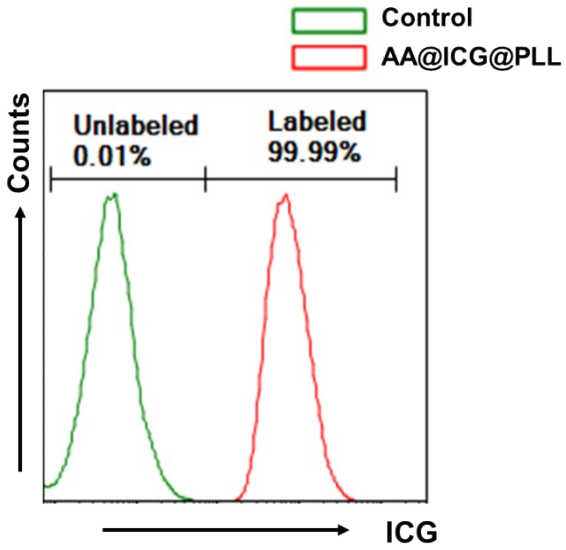

Figure S3. The evaluation of AA@ICG@PLL labeling efficiency.

A. Semiquantification of the AA@ICG@PLL-labeled area of MSCs with different Au concentrations. **B.** Flow cytometry analysis of BMSCs incubated with Au@ICG@PLL (200 μg mL^{-1} Au) for 24 h. The cells without Au@ICG@PLL labeling were examined as a control.

Supplementary Figure S4.

A.

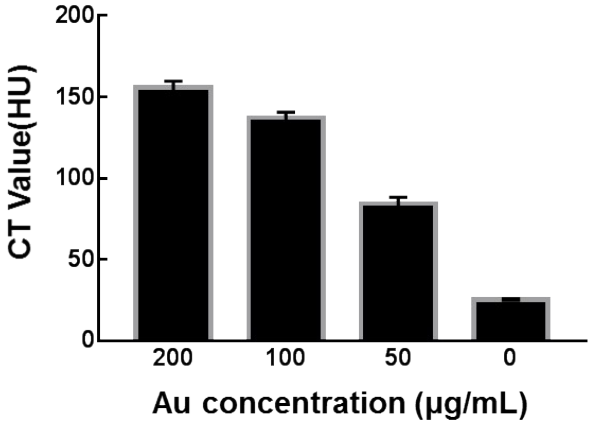

B.

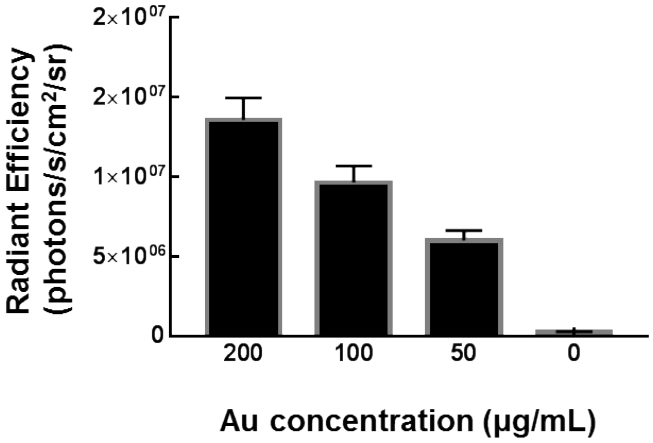

Figure S4. *In vitro* imaging ability of AA@ICG@PLL labeled BMSCs.

A. Calculated HU values of labeled BMSCs with various Au concentrations are shown in the bar chart. **B.** The total radiant efficiency of labeled BMSCs with various Au concentrations is shown in the bar chart.

Supplementary Figure S5.

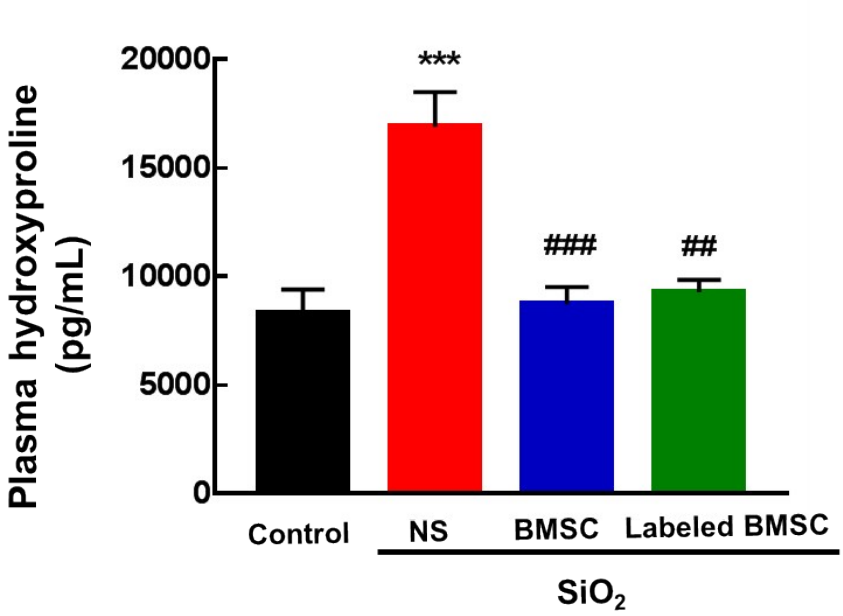

Figure S5. Plasma hydroxyproline content (pg/mL) of mice in each group on d28: control, SiO_2+NS, SiO_2+BMSC, and SiO_2+labeled BMSC groups. $^{***}p < 0.001$ compared with the control group. $^{###}p < 0.001$, $^{##}p < 0.01$ compared with the SiO_2+NS group.

Supplementary Figure S6.

A.

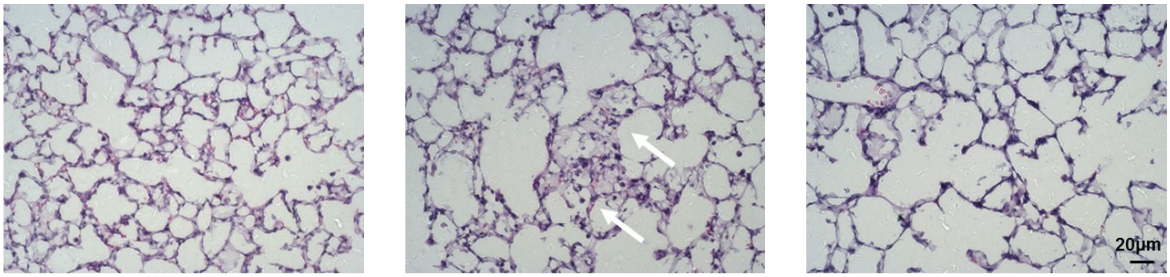

B.

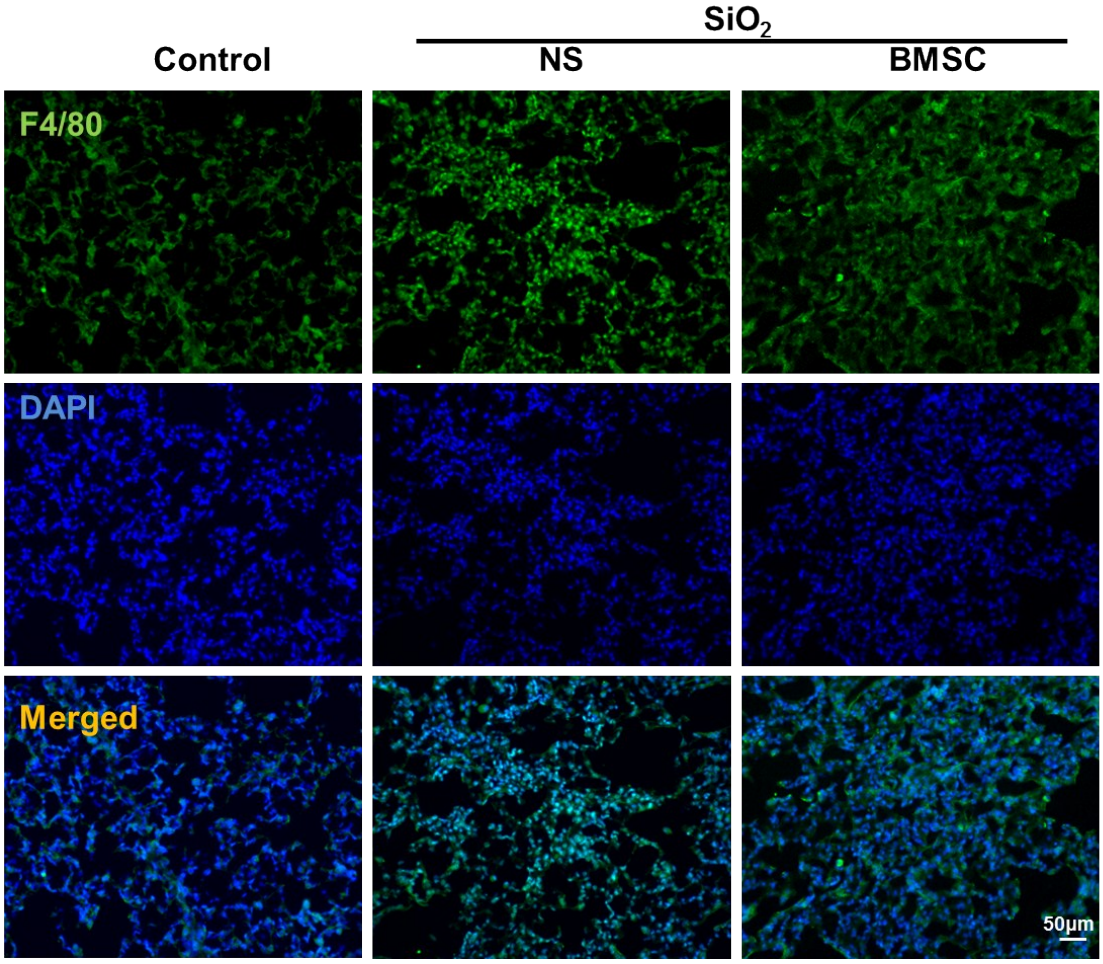

Figure S6. Lung histopathology on the 28th day after silica exposure in the control, SiO_2+NS, and SiO_2+BMSC groups. A. H&E staining of lung tissue, arrows indicate the aggregation of inflammatory cells. Scale bar = 20 μm. **B.** Immunohistochemistry of the macrophage marker F4/80 in lung tissues

from different groups. The images are representative of several sections in each group (n = 6). Scale bar=50 μm.

Supplementary Figure S7

A.

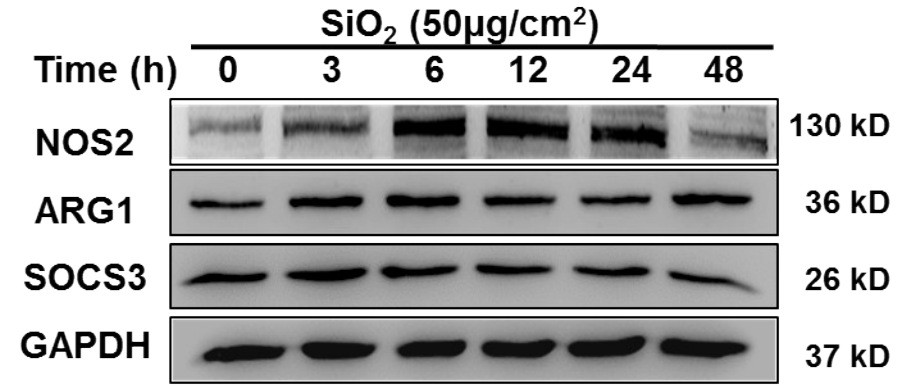

B.

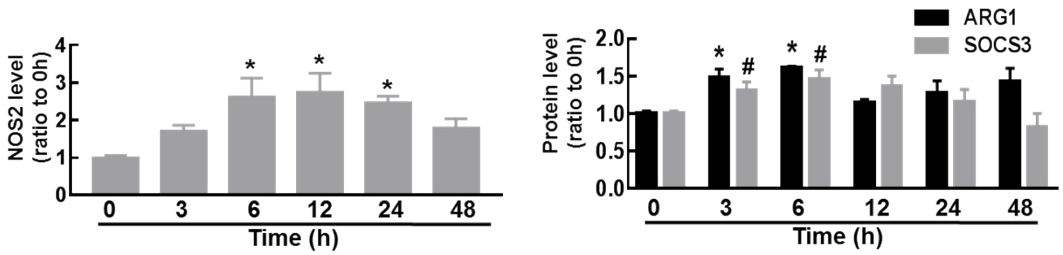

Figure S7. The effect of SiO_2 on the expression of the macrophage activation markers NOS2, ARG1, and SOCS3 in THP-1-derived macrophages.

A. Representative Western blots showing the effects of SiO_2 (50 μg/cm^2) on the expression of the M1 marker NOS2, the M2a marker ARG1, and the M2c marker SOCS3 in THP-1-derived macrophages. B. Densitometric analyses of Western blots from 3 separate experiments suggested that SiO_2 induced NOS2, ARG1, and SOCS3 expression in a time-dependent manner (n = 3); *$p < 0.05$, #$p < 0.05$ compared with the 0 h group.

Supplementary Movie S1

Movie S1. BMSCs took up AA@ICG@PLL NPs. Live-cell imaging demonstrated that AA@ICG@PLL NPs were loaded into the BMSC cytoplasm with prolonged incubation.

Supplementary Movie S2

Movie S2. Live-cell imaging revealed the migration and division of AA@ICG@PLL-labeled BMSCs over 24 h. Scale bar=20 μm.